

Electroexcitation of the Roper resonance for $1.7 < Q^2 < 4.5 \text{ GeV}^2$ in $\vec{e}p \rightarrow en\pi^+$

I.G. Aznauryan,^{1,2} V.D. Burkert,¹ W. Kim,⁴ K. Park,^{3,4} G. Adams,³⁶ M.J. Amarian,³⁴ P. Ambrozewicz,¹⁸ M. Anghinolfi,²⁴ G. Asryan,² H. Avakian,¹ H. Bagdasaryan,^{2,34} N. Baillie,⁴³ J.P. Ball,⁶ N.A. Baltzell,³ S. Barrow,¹⁹ V. Batourine,⁴ M. Battaglieri,²⁴ I. Bedlinskiy,²⁶ M. Bektasoglu,³⁴ M. Bellis,⁹ N. Benmouna,²⁰ B.L. Berman,²⁰ A.S. Biselli,^{36,9,17} L. Blaszczczyk,¹⁹ B.E. Bonner,³⁷ C. Bookwalter,¹⁹ S. Bouchigny,²⁵ S. Boiarinov,^{26,1} R. Bradford,⁹ D. Branford,¹⁵ W.J. Briscoe,²⁰ W.K. Brooks,^{14,1} S. Bültmann,³⁴ C. Butuceanu,⁴³ J.R. Calarco,³¹ S.L. Careccia,³⁴ D.S. Carman,¹ L. Casey,¹⁰ A. Cazes,³ S. Chen,¹⁹ L. Cheng,¹⁰ P.L. Cole,^{1,10,22} P. Collins,⁶ P. Coltharp,¹⁹ D. Cords,^{1,*} P. Corvisiero,²⁴ D. Crabb,⁴² V. Crede,¹⁹ J.P. Cummings,³⁶ D. Dale,²² N. Dashyan,² R. De Masi,^{11,25} R. De Vita,²⁴ E. De Sanctis,²³ P.V. Degtyarenko,¹ H. Denizli,³⁵ L. Dennis,¹⁹ A. Deur,¹ S. Dhamija,¹⁸ K.V. Dharmawardane,³⁴ K.S. Dhuga,²⁰ R. Dickson,⁹ C. Djalali,³ G.E. Dodge,³⁴ J. Donnelly,²¹ D. Doughty,^{12,1} M. Dugger,⁶ S. Dytman,³⁵ O.P. Dzyubak,³ H. Egiyan,^{31,1} K.S. Egiyan,^{2,*} L. El Fassi,⁵ L. Elouadrhiri,¹ P. Eugenio,^{9,19} R. Fatemi,⁴² G. Fedotov,³⁰ G. Feldman,²⁰ R.J. Feuerbach,⁹ T.A. Forest,^{34,22} A. Fradi,²⁵ H. Funsten,^{43,*} M.Y. Gabrielyan,¹⁸ M. Garçon,¹¹ G. Gavalian,^{31,34} N. Gevorgyan,² G.P. Gilfoyle,³⁸ K.L. Giovanetti,²⁷ F.X. Girod,^{11,1} J.T. Goetz,⁷ W. Gohn,¹³ E. Golovatch,^{30,24} A. Gonenc,¹⁸ C.I.O. Gordon,²¹ R.W. Gothe,³ L. Graham,³ K.A. Griffioen,⁴³ M. Guidal,²⁵ M. Guillo,³ N. Guler,³⁴ L. Guo,¹ V. Gyurjyan,¹ C. Hadjidakis,²⁵ K. Hafidi,⁵ K. Hafnaoui,⁵ H. Hakobyan,² R.S. Hakobyan,¹⁰ C. Hanretty,¹⁹ J. Hardie,^{12,1} N. Hassall,²¹ D. Heddle,¹ F.W. Hersman,³¹ K. Hicks,³³ I. Hleiqawi,³³ M. Holtrop,³¹ C.E. Hyde,³⁴ Y. Ilieva,^{3,20} D.G. Ireland,²¹ B.S. Ishkhanov,³⁰ E.L. Isupov,³⁰ M.M. Ito,¹ D. Jenkins,⁴¹ H.S. Jo,²⁵ J.R. Johnstone,²¹ K. Joo,^{13,42} H.G. Juengst,^{20,34} N. Kalantarians,³⁴ D. Keller,³³ J.D. Kellie,²¹ M. Khandaker,³² K.Y. Kim,³⁵ A. Klein,³⁴ F.J. Klein,^{18,10} A.V. Klimenko,³⁴ M. Kossov,²⁶ Z. Krahn,⁹ L.H. Kramer,^{18,1} V. Kubarovskiy,^{1,36} J. Kuhn,^{36,9} S.E. Kuhn,³⁴ S.V. Kuleshov,²⁶ V. Kuznetsov,⁴ J. Lachniet,^{9,34} J.M. Laget,^{11,1} J. Langheinrich,³ D. Lawrence,²⁹ T. Lee,³¹ Ji Li,³⁶ A.C.S. Lima,²⁰ K. Livingston,²¹ H.Y. Lu,³ K. Lukashin,¹⁰ M. MacCormick,²⁵ N. Markov,¹³ P. Mattione,³⁷ S. McAleer,¹⁹ B. McKinnon,²¹ J.W.C. McNabb,⁹ B.A. Mecking,¹ S. Mehrabyan,³⁵ J.J. Melone,²¹ M.D. Mestayer,¹ C.A. Meyer,⁹ T. Mibe,³³ K. Mikhailov,²⁶ R. Minehart,⁴² M. Mirazita,²³ R. Miskimen,²⁹ V. Mokeev,^{30,1} L. Morand,¹¹ B. Moreno,²⁵ K. Moriya,⁹ S.A. Morrow,^{25,11} M. Moteabbed,¹⁸ J. Mueller,³⁵ E. Munevar,²⁰ G.S. Mutchler,³⁷ P. Nadel-Turonski,²⁰ R. Nasseripour,^{20,3} S. Niccolai,^{20,25} G. Niculescu,^{33,27} I. Niculescu,^{20,1,27} B.B. Niczyporuk,¹ M.R. Niroula,³⁴ R.A. Niyazov,^{34,1} M. Nozar,^{39,1} G.V. O'Rielly,²⁰ M. Osipenko,²⁴ A.I. Ostrovidov,¹⁹ S. Park,¹⁹ E. Pasyuk,⁶ C. Paterson,²¹ S. Anefalos Pereira,²³ S.A. Phillips,²⁰ J. Pierce,⁴² N. Pivnyuk,²⁶ D. Pocanic,⁴² O. Pogorelko,²⁶ E. Polli,²³ I. Popa,²⁰ S. Pozdniakov,²⁶ B.M. Preedom,³ J.W. Price,⁸ Y. Prok,^{28,12,1} D. Protopopescu,^{31,21} L.M. Qin,³⁴ B.A. Raue,^{18,1} G. Riccardi,¹⁹ G. Ricco,²⁴ M. Ripani,²⁴ B.G. Ritchie,⁶ G. Rosner,²¹ P. Rossi,²³ D. Rowntree,²⁸ P.D. Rubin,³⁸ F. Sabatié,^{34,11} M.S. Saini,¹⁹ J. Salamanca,²² C. Salgado,³² J.P. Santoro,^{10,1} V. Sapunenko,^{24,1} D. Schott,¹⁸ R.A. Schumacher,⁹ V.S. Serov,²⁶ Y.G. Sharabian,¹ D. Sharov,³⁰ J. Shaw,²⁹ N.V. Shvedunov,³⁰ A.V. Skabelin,²⁸ E.S. Smith,¹ L.C. Smith,⁴² D.I. Sober,¹⁰ D. Sokhan,¹⁵ A. Stavinsky,²⁶ S.S. Stepanyan,⁴ S. Stepanyan,¹ B.E. Stokes,¹⁹ P. Stoler,³⁶ I.I. Strakovsky,²⁰ S. Strauch,³ R. Suleiman,²⁸ M. Taiuti,²⁴ T. Takeuchi,¹⁹ D.J. Tedeschi,^{3,16} A. Tkabladze,^{33,20} S. Tkachenko,³⁴ L. Todor,^{9,38} C. Tur,³ M. Ungaro,^{36,13} M.F. Vineyard,^{40,38} A.V. Vlassov,²⁶ D.P. Watts,^{15,21} L.B. Weinstein,³⁴ D.P. Weygand,¹ M. Williams,⁹ E. Wolin,¹ M.H. Wood,^{29,3} A. Yegneswaran,¹ J. Yun,³⁴ M. Yurov,⁴ L. Zana,³¹ B. Zhang,²⁸ J. Zhang,³⁴ B. Zhao,¹³ and Z.W. Zhao³

(The CLAS Collaboration)

¹Thomas Jefferson National Accelerator Facility, Newport News, Virginia 23606

²Yerevan Physics Institute, 375036 Yerevan, Armenia

³University of South Carolina, Columbia, South Carolina 29208

⁴Kyungpook National University, Daegu 702-701, Republic of Korea

⁵Argonne National Laboratory, Argonne, Illinois 60439

⁶Arizona State University, Tempe, Arizona 85287-1504

⁷University of California at Los Angeles, Los Angeles, California 90095-1547

⁸California State University, Dominguez Hills, Carson, California 90747

⁹Carnegie Mellon University, Pittsburgh, Pennsylvania 15213

¹⁰Catholic University of America, Washington, D.C. 20064

¹¹CEA-Saclay, Service de Physique Nucléaire, 91191 Gif-sur-Yvette, France

¹²Christopher Newport University, Newport News, Virginia 23606

¹³University of Connecticut, Storrs, Connecticut 06269

¹⁴Universidad Técnica Federico Santa María, Casilla 110-V, Valparaíso, Chile

- ¹⁵ *Edinburgh University, Edinburgh EH9 3JZ, United Kingdom*
¹⁶ *Emmy-Noether Foundation, Germany*
¹⁷ *Fairfield University, Fairfield, Connecticut 06824*
¹⁸ *Florida International University, Miami, Florida 33199*
¹⁹ *Florida State University, Tallahassee, Florida 32306*
²⁰ *The George Washington University, Washington, D.C. 20052*
²¹ *University of Glasgow, Glasgow G12 8QQ, United Kingdom*
²² *Idaho State University, Pocatello, Idaho 83209*
²³ *INFN, Laboratori Nazionali di Frascati, 00044 Frascati, Italy*
²⁴ *INFN, Sezione di Genova, 16146 Genova, Italy*
²⁵ *Institut de Physique Nucleaire ORSAY, Orsay, France*
²⁶ *Institute of Theoretical and Experimental Physics, Moscow, 117259, Russia*
²⁷ *James Madison University, Harrisonburg, Virginia 22807*
²⁸ *Massachusetts Institute of Technology, Cambridge, Massachusetts 02139-4307*
²⁹ *University of Massachusetts, Amherst, Massachusetts 01003*
³⁰ *Moscow State University, General Nuclear Physics Institute, 119899 Moscow, Russia*
³¹ *University of New Hampshire, Durham, New Hampshire 03824-3568*
³² *Norfolk State University, Norfolk, Virginia 23504*
³³ *Ohio University, Athens, Ohio 45701*
³⁴ *Old Dominion University, Norfolk, Virginia 23529*
³⁵ *University of Pittsburgh, Pittsburgh, Pennsylvania 15260*
³⁶ *Rensselaer Polytechnic Institute, Troy, New York 12180-3590*
³⁷ *Rice University, Houston, Texas 77005-1892*
³⁸ *University of Richmond, Richmond, Virginia 23173*
³⁹ *TRIUMF, 4004, Wesbrook Mall, Vancouver, BC, V6T 2A3, Canada*
⁴⁰ *Union College, Schenectady, New York 12308*
⁴¹ *Virginia Polytechnic Institute and State University, Blacksburg, Virginia 24061-0435*
⁴² *University of Virginia, Charlottesville, Virginia 22901*
⁴³ *College of William and Mary, Williamsburg, Virginia 23187-8795*

(Dated: March, 31)

The helicity amplitudes of the electroexcitation of the Roper resonance are extracted for $1.7 < Q^2 < 4.5 \text{ GeV}^2$ from recent high precision JLab-CLAS cross section and longitudinally polarized beam asymmetry data for π^+ electroproduction on protons at $W = 1.15 - 1.69 \text{ GeV}$. The analysis is made using two approaches, dispersion relations and a unitary isobar model, which give consistent results. It is found that the transverse helicity amplitude $A_{1/2}$ for the $\gamma^* p \rightarrow \text{N}(1440)\text{P}_{11}$ transition, which is large and negative at $Q^2 = 0$, becomes large and positive at $Q^2 \simeq 2 \text{ GeV}^2$, and then drops slowly with Q^2 . The longitudinal helicity amplitude $S_{1/2}$, which was previously found from CLAS $\bar{e}p \rightarrow e p \pi^0, e n \pi^+$ data to be large and positive at $Q^2 = 0.4, 0.65 \text{ GeV}^2$, drops with Q^2 . Available model predictions for $\gamma^* p \rightarrow \text{N}(1440)\text{P}_{11}$ allow us to conclude that these results provide strong evidence in favor of $\text{N}(1440)\text{P}_{11}$ as a first radial excitation of the $3q$ ground state. The results of the present paper also confirm the conclusion of our previous analysis for $Q^2 < 1 \text{ GeV}^2$ that the presentation of $\text{N}(1440)\text{P}_{11}$ as a $q^3\text{G}$ hybrid state is ruled out.

The excitation of nucleon resonances in electromagnetic interactions has long been recognized as a sensitive source of information on the long- and short-range structure of the nucleon and its excited states in the domain of quark confinement. Constituent quark models (CQM) have been developed that relate electromagnetic resonance transition form factors to fundamental quantities, such as the quark confining potential. While this relationship is more direct for heavy quarks, even in the light quark sector such connections exist and may be probed by measuring transition form factors over a large range in photon virtuality Q^2 , which defines the space-time resolution of the probe.

The so-called Roper resonance, or $\text{N}(1440)\text{P}_{11}$, is the lowest excited state of the nucleon. In the CQM, the simplest and most natural assumption is that this is the first radial excitation of the $3q$ ground state. However,

calculations within the nonrelativistic CQM fail to reproduce even the sign of the transition photo-coupling amplitude [1]. Moreover, the mass of the state is more than 100 MeV lower than what is predicted in the CQM with gluon exchange interaction [2, 3]. More recent models that include also Goldstone boson exchange between quarks gave better agreement with the mass [4]. To deal with shortcomings of the quark model, alternative descriptions of $\text{N}(1440)\text{P}_{11}$ were developed, where this resonance is treated respectively as: a hybrid $q^3\text{G}$ state where the three quarks are bound together with a gluon [5, 6], a quark core dressed by a meson cloud [7, 8], and a dynamically generated πN resonance [9]; other models include $3q - q\bar{q}$ components, in particular a strong σN component (see Ref. [10] and references therein). Discrimination between these descriptions of the Roper resonance can provide deep insight into the underlying basic symmetries

and the structure of quark confinement.

The Q^2 dependence of the electromagnetic transition form factors is highly sensitive to different descriptions of the Roper state. However, until recently, the data base used to extract these form factors was almost exclusively based on π^0 production, and very limited in kinematical coverage. Also, the $\pi^0 p$ final state is dominated by the nearby isospin $\frac{3}{2}$ $\Delta(1232)P_{33}$ resonance, whereas the isospin $\frac{1}{2}$ Roper state couples more strongly to the $\pi^+ n$ channel. The CLAS Collaboration has now published a large body of precise differential cross sections and polarized beam asymmetries for the process $\bar{e}p \rightarrow en\pi^+$ in the range of invariant hadronic mass $W = 1.15 - 1.69$ GeV and photon virtuality $Q^2 = 1.7 - 4.5$ GeV², with full azimuthal and polar angle coverage [11]. In this Letter we report the results on the electroexcitation of the Roper resonance extracted from this large data set.

The approaches we used to analyze the data are fixed- t dispersion relations (DR) and a unitary isobar model (UIM). They were successfully employed in Refs. [12, 13, 14] for analyses of pion-photoproduction and low- Q^2 -electroproduction data.

The imaginary parts of the amplitudes in the DR and UIM approaches are determined mainly by s -channel resonance contributions that we parameterize in the usual Breit-Wigner form with energy-dependent widths. We also take into account inelastic channels in the form proposed in Ref. [15]. An exception was made for the $\Delta(1232)P_{33}$ resonance, which was treated differently. According to the phase-shift analyses of πN scattering, the πN amplitude corresponding to the $P_{33}(1232)$ resonance is elastic up to $W = 1.43$ GeV (see, for example, the latest GWU analyses [16, 17]). In combination with DR and Watson's theorem, this provides strict constraints on the multipole amplitudes $M_{1+}^{3/2}$, $E_{1+}^{3/2}$, $S_{1+}^{3/2}$ that correspond to the $\Delta(1232)P_{33}$ resonance. In particular, as was shown in Ref. [12], the W -dependence of $M_{1+}^{3/2}$ is close to that from the GWU analysis [18] at $Q^2 = 0$ if the same normalizations of the amplitudes at the resonance position are used. This constraint on the large $M_{1+}^{3/2}$ amplitude plays an important role in the reliable extraction of the $N(1440)P_{11}$ electroexcitation amplitudes, because the $\Delta(1232)P_{33}$ and $N(1440)P_{11}$ states are overlapping.

We have taken into account all resonances from the first, second, and third resonance regions. These are 4- and 3-star resonances $\Delta(1232)P_{33}$, $N(1440)P_{11}$, $N(1520)D_{13}$, $N(1535)S_{11}$, $\Delta(1600)P_{33}$, $\Delta(1620)S_{31}$, $N(1650)S_{11}$, $N(1675)D_{15}$, $N(1680)F_{15}$, $N(1700)D_{13}$, $\Delta(1700)D_{33}$, $N(1710)P_{11}$, and $N(1720)P_{13}$. For the masses, widths, and πN branching ratios of these resonances, we used the mean values of the data presented in the Review of Particle Physics (RPP) [19]. In particular for the Roper resonance, the values $M = 1.44$ GeV, $\Gamma = 0.35$ GeV, and $\beta_{\pi N} = 0.6$ were taken. Resonances of the fourth resonance region practically have no influ-

ence in the energy region under investigation and were not included.

For the values of Q^2 under consideration, the available $ep \rightarrow ep\pi^0$ data are related mostly to the $\Delta(1232)P_{33}$ resonance region [20, 21, 22]. The DESY data [23] at higher energies $W = 1.14 - 1.72$ GeV ($Q^2 \approx 3$ GeV²) have very limited angular coverage. Our analysis showed that the combined $ep \rightarrow ep\pi^0$ [20, 21, 22, 23] and $\bar{e}p \rightarrow en\pi^+$ [11] data give results that are very close to those obtained from the $\bar{e}p \rightarrow en\pi^+$ data [11] alone. For this reason, and also to avoid mixing data sets with different systematic uncertainties, in this letter we present the results for $N(1440)P_{11}$ obtained from the analysis of the $\bar{e}p \rightarrow en\pi^+$ data [11] only.

At each Q^2 available for $\bar{e}p \rightarrow en\pi^+$ [11], $Q^2 = 1.72, 2.05, 2.44, 2.91, 3.48, 4.16$ GeV², we performed two kinds of fits in both approaches: (i) The magnitudes of the helicity amplitudes corresponding to all resonances listed above were fitted. (ii) The transverse amplitudes for the members of the multiplet $[70, 1^-]$: $\Delta(1620)S_{31}$, $N(1650)S_{11}$, $N(1675)D_{15}$, $N(1700)D_{13}$, and $\Delta(1700)D_{33}$, were fixed according to the single quark transition model [24], which relates these amplitudes to those for $N(1520)D_{13}$ and $N(1535)S_{11}$; the longitudinal amplitudes of these resonances and the amplitudes of the resonances $\Delta(1600)P_{33}$ and $N(1710)P_{11}$, which have small photocouplings [18, 19] and are not seen in low Q^2 π and 2π electroproduction [14], were assumed to be zero. The results obtained for $\Delta(1232)P_{33}$, $N(1440)P_{11}$, $N(1520)D_{13}$, and $N(1535)S_{11}$ in the two fits were very close to each other. The amplitudes of the Roper resonance presented below are the average values of the results obtained in these fits. The uncertainties arising from the averaging procedure we will refer to as uncertainties (I). They were included in quadrature into the total systematic uncertainties.

The background of both approaches contains Born terms corresponding to the s - and u -channel nucleon exchanges and t -channel pion contribution, and depends, therefore, on the proton, neutron, and pion form factors. The background of the UIM contains also the ρ and ω t -channel exchanges [15] and, therefore, the contribution of the form factors $G_{\rho(\omega) \rightarrow \pi\gamma}(Q^2)$. All of these form factors, except the neutron electric and $G_{\rho(\omega) \rightarrow \pi\gamma}(Q^2)$ ones, are known in the region of Q^2 under investigation from existing experimental data. For the proton form factors we used the parameterizations found for the existing data in Ref. [25]. The neutron magnetic form factor and the pion form factor were taken from Refs. [26] and [27, 28, 29, 30], respectively. The neutron electric form factor, $G_{E_n}(Q^2)$, is measured up to $Q^2 = 1.45$ GeV² [31], and Ref. [31] presents a parameterization for all existing data on $G_{E_n}(Q^2)$ that we used for extrapolation of $G_{E_n}(Q^2)$ to $1.7 < Q^2 < 4.2$ GeV². In our final results we accounted for a systematic uncertainty assuming a 50% deviation from this parameteri-

zation. There are no measurements of the form factors $G_{\rho(\omega) \rightarrow \pi\gamma}(Q^2)$; however, investigations made using both QCD sum rules [32] and quark model [33] predict a Q^2 dependence of $G_{\rho(\omega) \rightarrow \pi\gamma}(Q^2)$ close to the dipole form factor $G_d(Q^2) = 1/(1 + \frac{Q^2}{0.71 \text{ GeV}^2})^2$. In our analysis we assumed that $G_{\rho(\omega) \rightarrow \pi\gamma}(Q^2) = G_d(Q^2)$, and introduced in our final results a systematic uncertainty that can arise from a 50% deviation from this assumption. All of these uncertainties, including those that arise from the measured proton, neutron, and pion form factors, were added in quadrature and will be referred to as systematic uncertainties (II) in our final results.

In Fig. 1, we present the comparison of our results with the experimental data for the lowest Legendre moments of the structure function $\sigma_T + \epsilon\sigma_L$ at $Q^2 = 2.05 \text{ GeV}^2$ [11]. The Legendre moment $D_0^{T+\epsilon L}$ is the $\cos\theta_\pi^*$ independent part of $\sigma_T + \epsilon\sigma_L$; it does not contain interference of different multipole amplitudes and is related to the sum of squares of these amplitudes. The resonance behavior of the multipole amplitudes is revealed in $D_0^{T+\epsilon L}$ in the form of enhancements. Resonance structures related to the resonances $\Delta(1232)P_{33}$, $N(1520)D_{13}$, and $N(1535)S_{11}$ are clearly seen in $D_0^{T+\epsilon L}$. There is a shoulder between the Δ and 1.5 GeV peaks, which is related to the broad Roper resonance. To demonstrate this, we present in Fig. 1 the curves obtained by switching off the $N(1440)P_{11}$ resonance in the final DR results. A fit to the data with the Roper amplitudes put to zero results in $\chi^2 \approx 7$ and gives the dip in $D_0^{T+\epsilon L}$ of the same size as in Fig. 1. This clearly shows that the data can not be explained without the Roper resonance.

To stress the advantage of the investigation of the Roper resonance in the reaction $\gamma^*p \rightarrow \pi^+n$, we note that for this reaction the relative contribution of $N(1440)P_{11}$ in comparison with $\Delta(1232)P_{33}$ in $D_0^{T+\epsilon L}$ is four times larger than for $\gamma^*p \rightarrow \pi^0p$, because isospin $I = \frac{1}{2}$ and $\frac{3}{2}$ resonances enter the $ep \rightarrow eN\pi$ amplitudes with the coefficients $\sqrt{\frac{2}{3}}$, $\sqrt{\frac{1}{3}}$ for $n\pi^+$ in the final state and $-\sqrt{\frac{1}{3}}$, $\sqrt{\frac{2}{3}}$ for $p\pi^0$.

The role of $N(1440)P_{11}$ is also seen in other Legendre moments. In $D_1^{T+\epsilon L}$, the large effect caused by switching off this resonance is connected with the interference of

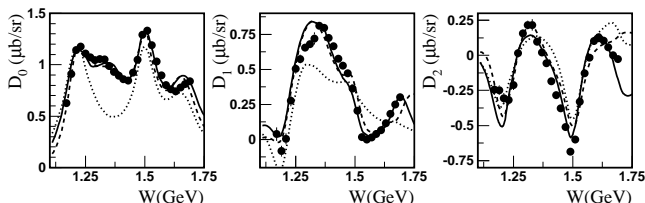


FIG. 1: Experimental data for the 3 lowest Legendre moments of the structure function $\sigma_T + \epsilon\sigma_L$ at $Q^2 = 2.05 \text{ GeV}^2$ [11] in comparison with our results. The solid and dashed curves correspond to the DR and UIM results, respectively. The dotted curves are obtained by switching off the $N(1440)P_{11}$ resonance in the final DR results.

Q^2 (GeV^2)	$A_{1/2}$ ($10^{-3}\text{GeV}^{-1/2}$)	$S_{1/2}$ ($10^{-3}\text{GeV}^{-1/2}$)	N_{data}	χ^2/N_{data}
DR				
1.72	$72.5 \pm 1.0 \pm 4.3$	$24.8 \pm 1.4 \pm 5.3$	5101	3.1
2.05	$72.0 \pm 0.9 \pm 4.2$	$21.0 \pm 1.7 \pm 5.0$	5844	2.4
2.44	$50.0 \pm 1.0 \pm 3.2$	$9.3 \pm 1.3 \pm 4.1$	6177	2.1
2.91	$37.5 \pm 1.1 \pm 2.8$	$9.8 \pm 2.0 \pm 2.3$	6251	2.0
3.48	$29.6 \pm 0.8 \pm 2.7$	$4.2 \pm 2.5 \pm 2.3$	6105	1.5
4.16	$19.3 \pm 2.0 \pm 3.9$	$10.8 \pm 2.8 \pm 4.5$	5778	1.1
UIM				
1.72	$58.5 \pm 1.1 \pm 4.2$	$26.9 \pm 1.3 \pm 5.3$	5101	3.5
2.05	$62.9 \pm 0.9 \pm 3.3$	$15.5 \pm 1.5 \pm 4.9$	5844	2.3
2.44	$56.2 \pm 0.9 \pm 3.2$	$11.8 \pm 1.4 \pm 4.1$	6177	2.1
2.91	$42.5 \pm 1.1 \pm 2.8$	$13.8 \pm 2.1 \pm 2.3$	6251	2.2
3.48	$32.6 \pm 0.9 \pm 2.6$	$14.1 \pm 2.4 \pm 2.0$	6105	1.6
4.16	$23.1 \pm 2.2 \pm 4.8$	$17.5 \pm 2.6 \pm 5.5$	5778	1.1

TABLE I: The $\gamma^*p \rightarrow N(1440)P_{11}$ helicity amplitudes found from the analysis of π^+ electroproduction data [11] using DR and UIM. The first and second uncertainties are, respectively, the statistical uncertainty from the fit and the systematic uncertainties (I) and (II) added in quadrature. The number of data points, N_{data} , and the χ^2 value per data point are also presented.

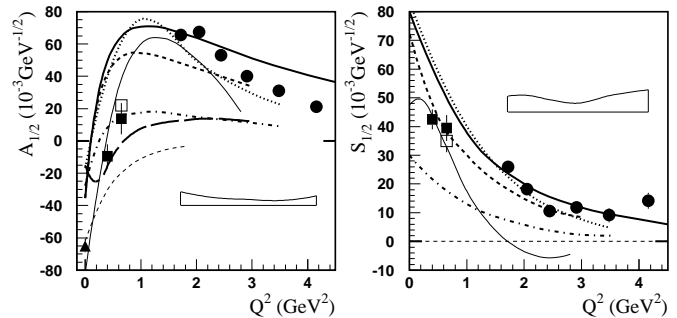


FIG. 2: Helicity amplitudes for the $\gamma^*p \rightarrow N(1440)P_{11}$ transition. The full circles are our results obtained from the analysis of π^+ electroproduction data [11]. The bands present the systematic uncertainties (I,II,III) added in quadrature; see text. The full boxes are the results obtained from CLAS data [13, 21, 34, 35, 36]; open boxes present the results of the combined analysis of CLAS single π and 2π electroproduction data [14]. The full triangle at $Q^2 = 0$ is the RPP estimate [19]. The thick curves correspond to the light-front relativistic quark models: dotted, dashed, dash-dotted, long-dashed, and solid curves are from Refs. [1, 37, 38, 39, 40], respectively. The thin solid curves are the predictions obtained for the Roper resonance treated as a quark core dressed by a meson cloud [7, 8]. The thin dashed curves are obtained assuming that $N(1440)P_{11}$ is a q^3G hybrid state [6].

M_{1-} corresponding to $N(1440)P_{11}$ with the non-resonant and $N(1535)S_{11}$ contributions to E_{0+} , which creates a linear dependence of $\sigma_T + \epsilon\sigma_L$ in $\cos\theta_\pi^*$. Due to interference effects like those mentioned above and to the large width of this state, the $N(1440)P_{11}$ plays a significant role in the entire W range covered by the data.

We now discuss the results for the $\gamma^*p \rightarrow N(1440)P_{11}$

helicity amplitudes presented in Table I and Fig. 2. The results obtained using DR and UIM are given in Table I separately; it can be seen that they are close to each other. As the non-resonant background of these approaches is built in conceptually different ways, we conclude that the model uncertainties of the obtained results are relatively small. In Fig. 2 we present average values of the results obtained within the DR and UIM approaches. The uncertainties that originate from this averaging procedure are referred to as systematic uncertainties (III) in our final results.

Combined with the information obtained from the previous CLAS data at $Q^2 = 0.4, 0.65 \text{ GeV}^2$ [13, 14, 21, 34, 35, 36], and that at $Q^2 = 0$ [19], our results show the following behavior of the transverse helicity amplitude $A_{1/2}$: being large and negative at $Q^2 = 0$, it crosses zero between $Q^2 = 0.4$ and 0.65 GeV^2 and becomes large and positive at $Q^2 \simeq 2 \text{ GeV}^2$. With increasing Q^2 , this amplitude drops smoothly in magnitude. The longitudinal helicity amplitude $S_{1/2}$, which is large and positive at small Q^2 , drops smoothly with increasing Q^2 .

In Fig. 2, we compare our results with model predictions. These are (i) quark model predictions [1, 37, 38, 39, 40] where the $N(1440)P_{11}$ is described as the first radial excitation of the $3q$ ground state; (ii) those assuming the $N(1440)P_{11}$ is a hybrid state [6]; and (iii) the results for the Roper resonance treated as a quark core (which is a radial excitation of the $3q$ ground state) dressed by a meson cloud [7, 8].

It is known that with increasing Q^2 , when the momentum transfer becomes larger than the masses of the constituent quarks, a relativistic treatment of the electroexcitation of the nucleon resonances, which is important already at $Q^2 = 0$, becomes crucial. A consistent way to perform the relativistic treatment of the $\gamma^*N \rightarrow N^*$ transitions is to consider them in light-front (LF) dynamics. In Fig. 2 we present the results obtained in the LF quark models [1, 37, 38, 39, 40]. All LF approaches [1, 37, 38, 39, 40] give a good description of nucleon form factors, however, the predictions for the $\gamma^*N \rightarrow N(1440)P_{11}$ helicity amplitudes differ significantly. This is caused by the large sensitivity of these amplitudes to the N and $N(1440)P_{11}$ wave functions [40]. The approaches [1, 37, 38, 39, 40] fail to describe the value of the transverse amplitude $A_{1/2}$ at $Q^2 = 0$. This can be an indication of a large meson cloud contribution to $\gamma^*p \rightarrow N(1440)P_{11}$, which is expected to be significant at small Q^2 . As a confirmation of this assumption, one can consider the results of Refs. [7, 8] where this contribution is taken into account, and a good description of the helicity amplitudes is obtained at small Q^2 .

In spite of the differences, all LF predictions for the $\gamma^*p \rightarrow N(1440)P_{11}$ helicity amplitudes have common features that agree with the results extracted from the experimental data: (i) the sign of the transverse amplitude $A_{1/2}$ at $Q^2 = 0$ is negative, (ii) the sign of the longi-

tudinal amplitude $S_{1/2}$ is positive, (iii) all LF approaches predict the sign change of the transverse amplitude $A_{1/2}$ at small Q^2 . We take this qualitative agreement as evidence in favor of the $N(1440)P_{11}$ resonance as a radial excitation of the $3q$ ground state. Final confirmation of this conclusion requires a complete simultaneous description of the nucleon form factors and the $\gamma^*p \rightarrow N(1440)P_{11}$ amplitudes. This will allow us to find the magnitude of the meson cloud contribution, and to better specify the N and $N(1440)P_{11}$ wave functions. To achieve a satisfactory description at large Q^2 , it may be necessary to take into account quark form factors, as well as other effects, such as the quark mass dependence on the momentum transfer.

The results of Refs. [5, 6], where $N(1440)P_{11}$ is treated as a hybrid state, are obtained via non-relativistic calculations. Nevertheless the suppression of the longitudinal amplitude $S_{1/2}$ has its physical origin in the fact that the longitudinal transition operator for the vertex $\gamma q \rightarrow qG$ requires both a spin and angular momentum flip by one unit, while the angular momenta of quarks in the N and $N(1440)P_{11} \equiv q^3G$ are equal to 0. This makes this result practically independent of relativistic effects. The predicted suppression of the longitudinal amplitude $S_{1/2}$ strongly disagrees with the experimental results.

In summary, for the first time the transverse and longitudinal helicity amplitudes of the $\gamma^*p \rightarrow N(1440)P_{11}$ transition are extracted from experimental data at high Q^2 . The results are obtained from differential cross sections and longitudinally polarized beam asymmetries for π^+ electroproduction on protons at $W = 1.15 - 1.69 \text{ GeV}$ [11]. The data were analyzed using two conceptually different approaches, DR and UIM, which give close results.

Comparison with quark model predictions provides strong evidence in favor of $N(1440)P_{11}$ as a first radial excitation of the $3q$ ground state.

The results for the longitudinal helicity amplitude confirm our conclusion made from the previous analysis of CLAS $\vec{e}p \rightarrow ep\pi^0, en\pi^+$ data for $Q^2 < 1 \text{ GeV}^2$ [13] that the presentation of the Roper resonance as a q^3G hybrid state is ruled out.

This work was supported in part by the U.S. Department of Energy and the National Science Foundation, the Korea Research Foundation, the French Commissariat a l'Energie Atomique, and the Italian Istituto Nazionale di Fisica Nucleare. Jefferson Science Associates, LLC, operates Jefferson Lab under U.S. DOE contract DE-AC05-06OR23177.

* Deceased

- [1] S. Capstick and B. D. Keister, Phys. Rev. D **51**, 3598 (1995).
- [2] S. Capstick and N. Isgur, Phys. Rev. D **34**, 2809 (1986).
- [3] J.-M. Richard, Phys. Rep. **212**, 1 (1992).

- [4] L. Ya. Glozman and D. O. Riska, *Phys. Rep.* **268**, 263 (1996).
- [5] Z. P. Li, *Phys. Rev. D* **44**, 2841 (1991).
- [6] Z. P. Li, V. Burkert, and Zh. Li, *Phys. Rev. D* **46**, 70 (1992).
- [7] F. Cano, P. González, S. Noguera, and B. Desplanques, *Nucl. Phys. A* **603**, 257 (1996).
- [8] F. Cano and P. González, *Phys. Lett. B* **431**, 270 (1998).
- [9] O. Kreil, C. Hanhart, S. Krewald, and J. Speth, *Phys. Rev. C* **62**, 025207 (2000).
- [10] M. Dillig and J. Schott, *Phys. Rev. C* **75**, 067001 (2007).
- [11] K. Park et al., CLAS Collaboration, *Phys. Rev. C* **77**, 015208 (2008).
- [12] I. G. Aznauryan, *Phys. Rev. C* **67**, 015209 (2003).
- [13] I. G. Aznauryan, V. D. Burkert, H. Egiyan, et al., *Phys. Rev. C* **71**, 015201 (2005).
- [14] I. G. Aznauryan, V. D. Burkert, et al., *Phys. Rev. C* **72**, 045201 (2005).
- [15] D. Drechsel, O. Hanstein, S. Kamalov, and L. Tiator, *Nucl. Phys. A* **645**, 145 (1999).
- [16] R. A. Arndt, W. J. Briscoe, I. I. Strakovsky, and R. L. Workman, *Phys. Rev. C* **69**, 035213 (2004).
- [17] R. A. Arndt, W. J. Briscoe, I. I. Strakovsky, and R. L. Workman, *Phys. Rev. C* **74**, 045205 (2006).
- [18] R. A. Arndt, W. J. Briscoe, I. I. Strakovsky, and R. L. Workman, *Phys. Rev. C* **66**, 055213 (2002).
- [19] W.-M. Yao et al. [Particle Data Group], *Journal of Physics G* **33**, 1 (2006).
- [20] V. V. Frolov et al., *Phys. Rev. Lett.* **82**, 45 (1999).
- [21] K. Joo et al., CLAS Collaboration, *Phys. Rev. Lett.* **88**, 122001 (2002).
- [22] M. Ungaro et al., CLAS Collaboration, *Phys. Rev. Lett.* **97**, 112003 (2006).
- [23] R. Haidan, PhD thesis, University of Hamburg, Hamburg, 1979.
- [24] V. D. Burkert et al., *Phys. Rev. C* **67**, 035204 (2003).
- [25] J. Arrington, W. Melnitchouk, and J. A. Tjon, *Phys. Rev. C* **76**, 035205 (2007).
- [26] W. K. Brooks et al., *Nucl. Phys. A* **755**, 261 (2005).
- [27] C. J. Bebek et al., *Phys. Rev. D* **13**, 25 (1976).
- [28] C. J. Bebek et al., *Phys. Rev. D* **17**, 1693 (1978).
- [29] T. Horn et al., *Phys. Rev. Lett.* **97**, 192001 (2006).
- [30] V. Tadevosyan et al., *Phys. Rev. C* **75**, 055205 (2007).
- [31] R. Madey et al., *Phys. Rev. Lett.* **91**, 122002 (2003).
- [32] V. Eletski and Ya. Kogan, *Yad. Fiz.* **39**, 138 (1984).
- [33] I. Aznauryan and K. Oganessyan, *Phys. Lett. B* **249**, 309 (1990).
- [34] K. Joo et al., CLAS Collaboration, *Phys. Rev. C* **68**, 032201 (2003).
- [35] K. Joo et al., CLAS Collaboration, *Phys. Rev. C* **70**, 042201 (2004).
- [36] H. Egiyan et al., CLAS Collaboration, *Phys. Rev. C* **73**, 025204 (2006).
- [37] H. J. Weber, *Phys. Rev. C* **41**, 2783 (1990).
- [38] F. Cardarelli, E. Pace, G. Salme, and S. Simula, *Phys. Lett. B* **397**, 13 (1997).
- [39] B. Juliá-Díaz, D. O. Riska, and F. Coester, *Phys. Rev. C* **69**, 035212 (2004).
- [40] I. G. Aznauryan, *Phys. Rev. C* **76**, 025212 (2007).